Research Article Vol. 29, No. 1 / 4 January 2021 / Optics Express 330
Optics EXPRESS

Coherent optical processes with an all-optical atomic simulator

IVAN A. BURENKOV,[1,2,*] IRINA NOVIKOVA,[3] OLGA V. TIKHONOVA,[4] AND SERGEY V. POLYAKOV[2,5]

[1]Joint Quantum Institute, Department of Physics, University of Maryland, College Park, MD 20742, USA
[2]National Institute of Standards and Technology, Gaithersburg, MD 20899, USA
[3]Department of Physics, College of William & Mary, Williamsburg, Virginia 23185, USA
[4]Moscow State University, Moscow 119991, Russia
[5]Department of Physics, University of Maryland, College Park, MD 20742, USA
[*]ivan.burenkov@gmail.com

Abstract: We show how novel photonic devices such as broadband quantum memory and efficient quantum frequency transduction can be implemented using three-wave mixing processes in a 1D array of nonlinear waveguides evanescently coupled to nearest neighbors. We do this using an analogy of an atom interacting with an external optical field using both classical and quantum models of the optical fields and adapting well-known coherent processes from atomic optics, such as electromagnetically induced transparency and stimulated Raman adiabatic passage to design. This approach allows the implementation of devices that are very difficult or impossible to implement by conventional techniques.

1. Introduction

In recent years, optical photonic chips have emerged as one of the most promising platforms for practical quantum computation. This technology reached an important milestone, demonstrating the "quantum supremacy" [1]. The all-optical photonic circuits are scalable [2] including the CMOS-compatibility [3] and potentially reprogrammable, enabling execution of a variety of algorithms on the same device. All-optical control via second order nonlinearity is significantly faster than other reprogramming methods and adds frequency as a synthetic dimension – a substantial improvement over arrays of linear evanescently-coupled waveguides. Second order nonlinearity enables three-wave mixing (TWM) [4], which includes a second harmonic generation (SHG) and a sum-/difference-frequency generation (SFG/DFG) [5]. Applications of TWM such as entanglement generation [6], quantum frequency conversion [7], and optical parametric oscillators [8,9] have been long-known. Compact and efficient off-the-shelf components for these applications are now readily available [10–16]. Recent advances in the fabrication of periodically-poled lithium niobate (PPLN) waveguides have allowed very high efficiency of TWM processes with optical propagation losses as low as 0.03 dB/cm [17,18].

Linear and nonlinear waveguide lattices, consisting of an array of evanescently coupled waveguides attracted a lot of attention [19–21]. For example, equations describing the propagation of optical fields in an array of identical straight waveguides evanescently coupled to their next neighbors have the same functional form as the Schrödinger equation, with conjugated field amplitudes representing wavefunction coefficients, and with the spatial evolution replacing the temporal one [22]. This model allows one to employ classical optics analogs of both non-relativistic and relativistic quantum mechanical systems [23]. In particular, this system was used to simulate displaced Fock states [24], W-states [25], and squeezed states [26]. Particularly, by using intensity correlations, it is possible to study the path-entanglement created by propagation of photonic lattices [27]. Waveguide arrays can also provide a classical platform for tight-binding models [28], Majorana physics [29] and the Jaynes-Cummings model [30].

Here we introduce a novel formalism in which classical and quantum optical fields in evanescently coupled waveguides with second-order nonlinearity can be arranged to model

#415480 https://doi.org/10.1364/OE.415480

Received 20 Nov 2020; revised 11 Dec 2020; accepted 12 Dec 2020; published 22 Dec 2020

Optics EXPRESS

atomic systems interacting with external optical fields. This approach reproduces the phenomena from a rich playbook of atomic quantum optics, such as electromagnetically induced transparency (EIT) and stimulated Raman adiabatic passage (STIRAP) [31], in a nonlinear photonic lattice with all-optical quantum states. In the proposed formalism, atomic levels are represented by spatial *and* spectral optical modes coupled to each other in a controlled manner by TWM nonlinear processes. In contrast to a real atomic system, one can engineer a true 2- or n-level model of the "atomic" system with varying complexity. For example, in the simplest case, all atomic levels can be made non-degenerate and spinless. Such "atomic" systems are not sensitive to external magnetic fields. At the same time, these systems can be tuned via temperature and via TWM nonlinear control.

Here we demonstrate a number of new photonic devices, inspired by the analogy with the atoms. For example, we show how an all-optical analog of EIT in the system of two evanescently coupled waveguides can be used as an ultrafast broadband all-optical switch or on-chip quantum memory. Similarly, a STIRAP optical analogy gives rise to the robust frequency transduction when direct frequency conversion is impractical. Key advantages of nonlinear coupling between modes over linear coupling are: (1) the coupling strength can be changed by the end-user simply by adjusting the pump power, (2) the coupled modes may have same or different frequencies, and (3) a synthetic spectral dimension can be added to the spatial dimension of a waveguide array.

2. Two-level atom analogy: three-wave mixing in a single nonlinear waveguide

In this section, we show that propagation dynamics of two optical fields and a pump mutually coupled via TWM in a nonlinear waveguide is equivalent to temporal dynamics of a two-level atom interacting with an external optical field. In the following calculations we assume that each waveguide supports a single spatial mode and multiple spectral modes. We mathematically describe the three-wave mixing (TWM) in such a waveguide using the plane-wave approximation, and note that complete energy conversion from one wavelength to another is theoretically possible [5]. Very high quantum SFG/DFG conversion efficiencies were demonstrated experimentally; for example nearly 100 % internal efficiency for the pulse conversion [32] and more than 80 % efficiency for continuous wave conversion [33,34], were demonstrated. A 100 % conversion has been approached even in a more challenging case of SHG, [35]. In the slowly varying amplitudes approximation and in the presence of a strong pump field A_p with frequency ω_p, evolution of an input optical field A_i with frequency ω_i and sum-frequency field A_s with frequency ω_s, can be written as [5]:

$$\begin{cases} \partial_z A_\mathrm{i} = \frac{2i\omega_\mathrm{i}^2 d_\mathrm{eff}}{k_\mathrm{i} c^2} A_\mathrm{p}^* A_\mathrm{s} e^{-i\Delta k z}, \\ \partial_z A_\mathrm{s} = \frac{2i\omega_\mathrm{s}^2 d_\mathrm{eff}}{k_\mathrm{s} c^2} A_\mathrm{p} A_\mathrm{i} e^{i\Delta k z}, \end{cases} \tag{1}$$

where $\omega_\mathrm{s} = \omega_\mathrm{i} + \omega_\mathrm{p}$, c is speed of light in vacuum, d_eff is the effective nonlinear coupling coefficient defined by nonlinear properties of the waveguide, and $\Delta k = k_\mathrm{i} + k_\mathrm{p} - k_\mathrm{s}$ is the phase mismatch. Here we use the propagation constants $k_\mathrm{i,s,p} = n_\mathrm{i,s,p}\omega_\mathrm{i,s,p}/c$, where $n_\mathrm{i,s,p}$ are the effective refractive indexes in the waveguides of the input, sum-frequency and pump optical modes, respectively. In the non-depleted pump approximation $\partial_z A_\mathrm{p} \approx 0$. By using the following substitutions:

$$\begin{aligned} \Omega/2 &= \tfrac{2d_\mathrm{eff}}{c} \left|A_\mathrm{p}\right| \sqrt{\omega_\mathrm{i}\omega_\mathrm{s}/(n_\mathrm{i}, n_\mathrm{s})}; \\ \phi &= \arg(A_\mathrm{p}); \\ A_\mathrm{i} &= C_\mathrm{i}\sqrt{\omega_\mathrm{i}/n_\mathrm{i}}; \\ A_\mathrm{s} &= C_\mathrm{s}\sqrt{\omega_\mathrm{s}/n_\mathrm{s}}, \end{aligned} \tag{2}$$

Optics EXPRESS

one can rewrite the system (1) as:

$$\begin{cases} \partial_z C_{\mathrm{i}} = i\frac{\Omega}{2} C_{\mathrm{s}} e^{-i\phi} e^{-i\Delta k z}, \\ \partial_z C_{\mathrm{s}} = i\frac{\Omega}{2} C_{\mathrm{i}} e^{i\phi} e^{i\Delta k z}. \end{cases} \tag{3}$$

These equations are mathematically identical to those describing Rabi oscillations of an idealized single two-level atom interacting with a single-mode classical field in the absence of dephasing. Here temporal evolution of atomic states is replaced by the spatial evolution of the optical modes during propagation in a nonlinear waveguide ($t \rightarrow z$), and Ω is equivalent to the atomic Rabi frequency, see Fig. 1. Notice that the average photon flux for input and sum-frequency fields can be written as:

$$\langle F \rangle_{\mathrm{i,s}} = \frac{I_{\mathrm{i,s}}}{\hbar\omega_{\mathrm{i,s}}} = \frac{2n_{\mathrm{i}} c\epsilon_0 \left|A_{\mathrm{i,s}}\right|^2}{\hbar\omega_{\mathrm{i,s}}} = 2c\epsilon_0 \left|C_{\mathrm{i,s}}\right|^2 .$$

Therefore, absolute squares of amplitudes $\left|C_{\mathrm{i,s}}\right|^2$ are proportional to the photon fluxes in the corresponding optical modes {i, s}. At the same time, in this all-optical analogy to the atomic system, $\left|C_{\mathrm{i,s}}\right|^2$ represent populations of the two states of the model two-level atom. Therefore, TWM process can be used for an all optical simulation of an atomic system, with the population of the "optical atomic states" directly mapping to photon flux. In other words, populations of all-optical atomic states are proportional to optical power in each mode, and thus can be measured using an optical power meter.

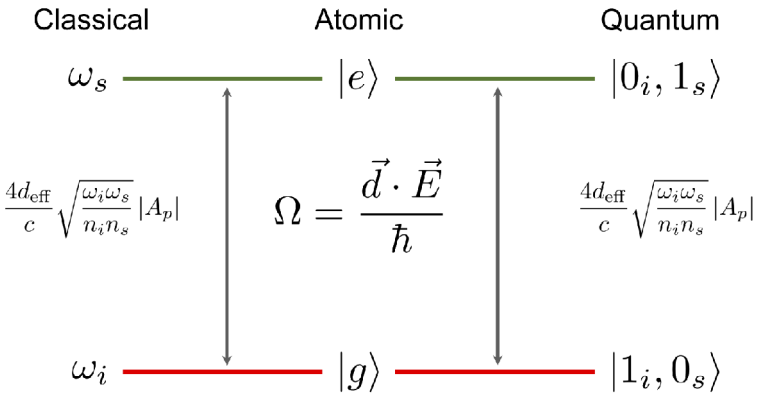

Fig. 1. The analogy between TWM of classical fields, the two-level atom interacting with an external field, and TWM of single-photon fields.

3. Quantum model of three-wave mixing in a nonlinear waveguide

The analogy introduced in the previous section can be extended to the quantum regime. We consider the extension of the theoretical model to a quantum description of the optical modes in the waveguide, except for the strong undepleted pump field(s) which we treat classically. The interaction Hamiltonian for the nonlinear waveguide describing TWM coupling between two quantized spectral modes for sum (s) and input (i) photons respectively is: [7]:

$$H = i\frac{2d_{\mathrm{eff}}\left|A_{\mathrm{p}}\right|}{c}\left(\frac{\omega_{\mathrm{i}}}{n_{\mathrm{i}}} e^{-i\phi} e^{-i\Delta k z} a_{\mathrm{i}}{}^{\dagger} a_{\mathrm{s}} + \frac{\omega_{\mathrm{s}}}{n_{\mathrm{s}}} e^{i\phi} e^{i\Delta k z} a_{\mathrm{s}}{}^{\dagger} a_{\mathrm{i}}\right). \tag{4}$$

Let us first consider the case of only one photon present in the system:

$$\psi(0) = \left(b_{|1_{\mathrm{i}},0_{\mathrm{s}}\rangle} a_{\mathrm{i}}{}^{\dagger} + b_{|0_{\mathrm{i}},1_{\mathrm{s}}\rangle} a_{\mathrm{s}}{}^{\dagger}\right)|0\rangle,$$

Optics EXPRESS

$$1 = |b_{|1_i,0_s\rangle}|^2 + |b_{|0_i,1_s\rangle}|^2.$$

In this case one can look for the solution of the non-stationary Schrödinger equation (NSE) in the following form:

$$\psi(z) = (b_{|1_i,0_s\rangle}(z)a_i^\dagger + b_{|0_i,1_s\rangle}(z)a_s^\dagger)|0\rangle.$$

By using the substitution (2) and projecting on the Fock basis, one can obtain the following system of equations for complex amplitudes $b_{i,s}$ for single-photon excitation in the nonlinear waveguide:

$$\begin{cases} \partial_z b_{|1_i,0_s\rangle} = i\frac{\Omega}{2} b_{|0_i,1_s\rangle} e^{-i\phi} e^{-i\Delta kz}, \\ \partial_z b_{|0_i,1_s\rangle} = i\frac{\Omega}{2} b_{|1_i,0_s\rangle} e^{i\phi} e^{i\Delta kz}. \end{cases}$$

Notice that these equations are identical to the semiclassical approach (3) after substitution $b_{|1_i,0_s\rangle} \rightarrow C_i$ and $b_{|0_i,1_s\rangle} \rightarrow C_s$ (Fig. 1). Thus, when only a single photon is present, fully quantum optical models of an atom are identical to their semi-classical counterparts. However, in the quantum regime, the "atomic" state populations now correspond to the populations of the single-photon states in signal and idler modes $\left|b_{|0_i,1_s\rangle}\right|^2$ and $\left|b_{|1_i,0_s\rangle}\right|^2$, rather than to the values of the photon flux in these modes. Therefore, the classical case is analogous to a simulation for mean values of atomic populations and coherences, while the single photon simulates experiments with single atoms, c.f. [21].

In the single-photon case we used the fact that only two states – $|1_i, 0_s\rangle$ and $|0_i, 1_s\rangle$ – exist in the waveguide, allowing their mapping into the Jaynes-Cummings states $|g, 1\rangle$ and $|e, 0\rangle$, where g and e are indexes of the ground and excited states of the atom, and "0" and "1" are the number of photons in each mode of the quantized optical field.

With more than one photon in the waveguide, all possible combinations of the two-mode Fock states $|n_i, n_s\rangle$ such that $n = n_i + n_s$ can be present in the waveguide. For $n = 2$, there are 3 possible combinations: $|2_i, 0_s\rangle$, $|0_i, 2_s\rangle$ and $|1_i, 1_s\rangle$. Using the Hamiltonian (4), one can obtain the following system of equations for complex amplitudes of these states:

$$\begin{cases} \partial_z b_{20} = i\frac{\Omega}{2}\sqrt{2} b_{11} e^{-i\phi} e^{-i\Delta kz}, \\ \partial_z b_{11} = i\frac{\Omega}{2}\sqrt{2}(b_{20} e^{i\phi} e^{i\Delta kz} + b_{02} e^{-i\phi} e^{-i\Delta kz}), \\ \partial_z b_{02} = i\frac{\Omega}{2}\sqrt{2} b_{11} e^{i\phi} e^{i\Delta kz}, \end{cases}$$

where we simplified the index notations $b_{|p_i,q_s\rangle} \Rightarrow b_{pq}$. In the case of two-photon excitation, a spectral NOON state with $N = 2$ is coupled to a biphoton state$|1_i, 1_s\rangle$, and equivalent to the Hong-Ou-Mandel effect in two coupled linear waveguides for two indistinguishable photons. For an arbitrary length of the waveguides the Hamiltonian is equivalent to a beamsplitter, but instead of splitting a beam in two spatial directions, the beam is splitted into two different spectral modes, c.f. [20].

4. Multi-level atoms model: evanescently-coupled waveguides and nonlinearly-coupled multiple optical modes

In a linear waveguide array evanescent coupling of a single spectral mode m in the j^{th} waveguide to its next neighbor is described by the system of ordinary differential equations [36]:

$$\partial_z A_j^m = i(c_{j,j+1}^m A_{j+1}^m + c_{j,j-1}^m A_{j-1}^m).$$

Similarly, the poling can be designed to phase-match more than just one set of TWM-coupled modes [37,38]. Thus, multiple coupled modes can co-exist in a single waveguide. In a full analogy with evanescent coupling, if several TWM processes are phase-matched, coupling between several spectral components can be induced by using multiple classical pumps. The advantages of this configuration are threefold. First, the coupling coefficients $\Omega_j^{lm}/2$, phases ϕ_j^{lm}

Optics EXPRESS

and phase mismatch Δk_j^{lm} can be controlled by tuning external classical pump fields. Second, coupled fields can have different wavelengths, which increases the range of practical devices that can be built based on this platform. Third, by combining the two types of coupling, we can take advantage of a synthetic dimension due to spectral modes. Particularly, a 1D array of physical waveguides becomes a quasi 2D array of coupled modes. Indeed, in the undepleted pump approximation, and using the substitution (2) for M spectral modes, one writes:

$$\begin{aligned} \partial_z C_j^m &= i\left(\Lambda_{j,j+1}^m C_{j+1}^m - \Lambda_{j,j-1}^m C_{j-1}^m\right) + \\ &+ i/2 \sum_{l\neq m} \Omega_j^{lm}(z) e^{\pm i\phi_j^{lm}} e^{\pm i\Delta k_j^{lm} z} C_j^l, \end{aligned}$$

where $\Omega_j^{lm}(z)/2$ is an effective TWM coupling coefficient (Rabi frequency) between m and l spectral modes in the j^{th} waveguide, $\Lambda_{j,j\pm1}^m = c_{j,j+1}^m\sqrt{\omega_m/n_m}$ is the effective evanescent coupling of spectral mode m between neighboring j^{th} and $(j+1)^{\text{th}}$ waveguides, and the positive (negative) argument of the exponent corresponds to the SFG (DFG) coupling. Note, that in this configuration the value of $\Omega_j^{lm}(z)$ can change with propagation parameter z, since the pump field can oscillate between the neighbor waveguides due to their evanescent coupling. One can take advantage of this effect to engineer Floquet-type interactions in the system [39]. Thus, in contrast with evanescently coupled arrays, taking advantage of the spectral domain allows the flexibility of using the same physical device to simulate different Hamiltonians.

Of particular interest here are novel devices that are inspired by coherent atomic phenomena. To this end, a three-level atom interacting with two classical fields enables an all-optical analog of the coherent population trapping (CPT), EIT, and STIRAP effects. We will describe practical photonic devices based on EIT and STIRAP using a small number of waveguides and pumps. We will also show that this 1D photonic system can emulate complex, multidimensional hamiltonians that typically occur in photonic lattices filled with cold atomic gases. Here we will present only the semiclassical description, since it can be straightforwardly extended to a single-photon case, as shown in the previous section.

4.1. All-optical EIT-inspired switch

Consider the simplest case of *two* waveguides $\{0,1\}$ with $\Lambda^m = \Lambda_{0,1}^m = \Lambda_{1,0}^m$ and *two* spectral modes {i,s} with $\Omega_{0,1} = \Omega_{0,1}^{\text{i,s}}/2$:

$$\begin{cases} i\partial_z C_0^{\text{i}} = -\Lambda^{\text{i}} C_1^{\text{i}} - \Omega_0 e^{-i\phi_0} e^{-i\Delta k_0 z} C_0^{\text{s}}, \\ i\partial_z C_0^{\text{s}} = -\Lambda^{\text{s}} C_1^{\text{i}} - \Omega_0 e^{i\phi_0} e^{i\Delta k_0 z} C_0^{\text{i}}, \\ i\partial_z C_1^{\text{i}} = -\Lambda^{\text{i}} C_0^{\text{i}} - \Omega_1 e^{-i\phi_1} e^{-i\Delta k_1 z} C_1^{\text{s}}, \\ i\partial_z C_1^{\text{s}} = -\Lambda^{\text{s}} C_0^{\text{s}} - \Omega_1 e^{i\phi_1} e^{i\Delta k_1 z} C_1^{\text{i}}, \end{cases}$$

For simplicity, we assume that wavelength $\lambda_{\text{s}} \ll \lambda_{\text{i}}$. Then $\Lambda^{\text{i}} \gg \Lambda^{\text{s}} \approx 0$ because modes with shorter wavelength are better confined. By using identical pump fields in both waveguides one can eliminate dependence of Ω on z. Further, assuming that TWM is phase-matched in only in the waveguide 1 (Fig. 2), the above equations can then be re-written as:

$$\begin{cases} i\partial_z C_0^{\text{i}}(z) = -\Lambda^{\text{i}} C_1^{\text{i}}, \\ i\partial_z C_1^{\text{i}}(z) = -\Lambda^{\text{i}} C_1^{\text{i}} - \Omega_1 e^{-i\phi_1} e^{-i\Delta k_1 z} C_1^{\text{s}}, \\ i\partial_z C_1^{\text{s}}(z) = -\Omega_1 e^{i\phi_1} e^{i\Delta k_1 z} C_1^{\text{i}}, \end{cases} \tag{5}$$

where we dropped the equation for C_0^{s} since it is decoupled from other modes. Following the analogy of all-optical atomic states, this photonic model can be interpreted as a three level

Optics EXPRESS

"atomic" system and therefore can be used to simulate EIT-like processes. In the absence of the pump, $C_1^{\mathrm{p}} = 0$, the idler field oscillates periodically between the two waveguides due to their evanescent coupling. By selecting an appropriate coupling constant Λ^i and length of the chip L, the input $\left|C_0^{\mathrm{i}}(0)\right|^2 = 1$, $\left|C_1^{\mathrm{i}}(0)\right|^2 = 0$ can be fully transferred into the other waveguide at the output: $\left|C_0^{\mathrm{i}}(L)\right|^2 = 0$, $\left|C_1^{\mathrm{i}}(L)\right|^2 = 1$. The pump field turns on the coupling between the spectral modes "i" and "s" in waveguide 1. Equations (5) show that a proper choice of the coupling constants suppresses the light transfer between the waveguides due to the EIT-like destructive interference. The results of numerical simulations for this system are shown in Fig. 3, where the nonlinear coupling strength $\Omega_1 = 0.23$ mm^{-1} corresponds to a modest pump power of ≈ 200 mW and the frequency conversion normalized efficiency $\eta = 2600\%$ W^{-1} cm^{-2}, values reported experimentally for nanophotonic PPLN waveguides [18]. The unique property of this effect is that both the input and the output remain at the same frequency (ω_{i}), while the control field can be significantly red-detuned from both the input and output frequencies to eliminate both Raman and SPDC noise in $LiNbO_3$ [12,13]. This system can be used in practice as an ultrafast all-optical switch for faint states of light. Its switching time is limited only by the bandwidth of the TWM process in the nonlinear waveguide, and thus can achieve sub-ps switching times [40].

A looped nonlinear waveguide with an integrated switch can store short broadband optical pulses, operating as an ultrafast and broadband quantum memory. For example, a single round trip delay of $L_{\mathrm{loop}}/(nc) \approx 1$ ns can be realized in a looped ≈ 7 cm-long waveguide (same as the expected nonlinear interaction length of the proposed switch). Due to the high internal losses (of the order of 0.03 dB/cm), the storage time in a lithium niobate waveguide loop device is limited to just a few ns. Longer storage times are achievable by employing low-loss materials such as silicon nitride [41] to fabricate the delay loop waveguide that is evanescently coupled to PPLN waveguide. This is because only one waveguide needs to be nonlinear for our EIT-like switching method to work.

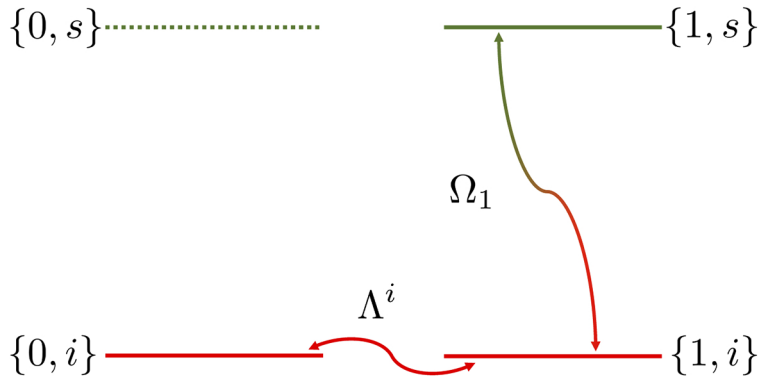

Fig. 2. Effective level configuration for EIT in two coupled waveguides supporting two spectral modes "i" and "s" with TWM in the waveguide #1.

4.2. *All-optical STIRAP for frequency conversion*

Another well-known effect in atomic optics is STIRAP. In STIRAP, the population is transferred between two atomic states via two sequential coherent pulses. Here we propose using the all-optical STIRAP for frequency conversion between the states that are hard to couple in a single-step TWM transduction. For example, the use of a blue detuned pump can be undesirable since it can result in significant background noise due to spontaneous parametric downconversion (SPDC) processes [33]. Alternatively, the two states can be spectrally too close to couple them directly using an accessible optical pump. Indeed, transduction between the two communication

Optics EXPRESS

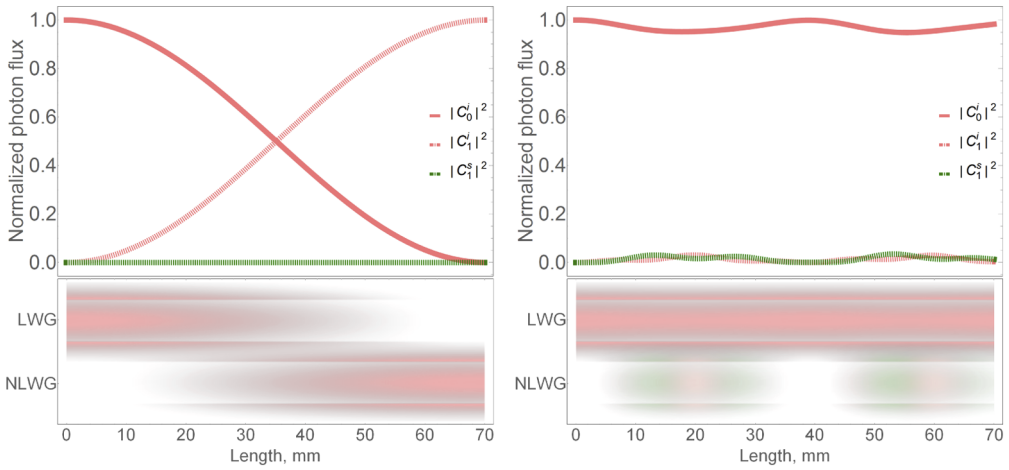

Fig. 3. A numerical simulation of photon flux in the ultrafast all-optical switch implemented with a coupled linear waveguide (LWG) and nonlinear waveguide (NLWG). In the absence of an optical control pump field, the signal field is transferred from LWG to NLWG (left). When the control field is applied, the signal field remains in LWG due to an EIT-like destructive interference (right). Bottom graphs show a conceptual layout of waveguides in the proposed experimental implementation (disproportionally scaled because waveguide width is of order of 1 μm); color gradients are the artistic representations of the switching process in coupled LWG and NLWG. Simulation parameters: $\Lambda^i = 0.1\Omega_1 = 0.023$ mm^{-1}, $\Delta k_1 = 0.15$ mm^{-1} (see text).

bands at 1310 nm and 1550 nm via TWM nonlinear frequency conversion requires a pump at 8.5 μm, but the transparency window in most TWM crystals is limited to $\lesssim 5$ μm in the infrared; the other choice is to use a 710 nm pump, but the SPDC background noise will be significant. If the strong pump is too close to one of the fields spectrally, significant background noise will be generated via Raman scattering. For instance, if transduction between the Rubidium transition at 780 nm (^{87}Rb D_2 ($5^2S_{1/2} \rightarrow 5^2P_{3/2}$)) and the telecommunication band at 1550 nm is desired, a strong pump at 1570 nm required, which is detuned by just 20 nm from one of the fields. The STIRAP approach allows coupling the two target spectral modes while avoiding practical limitations of TWM.

Two configurations are possible, depending on the frequencies of the participating optical fields. A Λ-configuration can be used to couple two spectrally close target fields (Fig. 4). A ladder configuration is desirable for spectrally distant target fields. In our first example above, one can couple the two communication bands via an intermediate "dark state" at $\approx$ 900 nm with the proposed STIRAP-like TWM using two commercially available pumps at $\approx$2.15 μm and $\approx$2.87 μm that conveniently occur within the transparency window of lithium niobate. The second example of Rb frequency transduction can be realized using an intermediate "dark state" at 1064 nm and two pumps at $\approx$ 2.9 μm and $\approx$ 3.4 μm.

The STIRAP-like evolution of the optical fields is described by the following system of differential equations:

$$\begin{cases} i\partial_z C_a(z) = -\Omega_{ab}(z)e^{i\Delta k_{ab}z}C_b, \\ i\partial_z C_b(z) = -\Omega_{ab}(z)e^{-i\Delta k_{ab}z}C_a - \Omega_{bc}(z)e^{\pm i\Delta k_{bc}z}C_c, \\ i\partial_z C_c(z) = -\Omega_{bc}(z)e^{\mp i\Delta k_{bc}z}C_b \end{cases}$$

where signs of the exponent's arguments are "+" in the second equation and "-" in the third equation for a Λ-configuration. For a ladder-configuration, these signs are flipped. To achieve

Optics EXPRESS

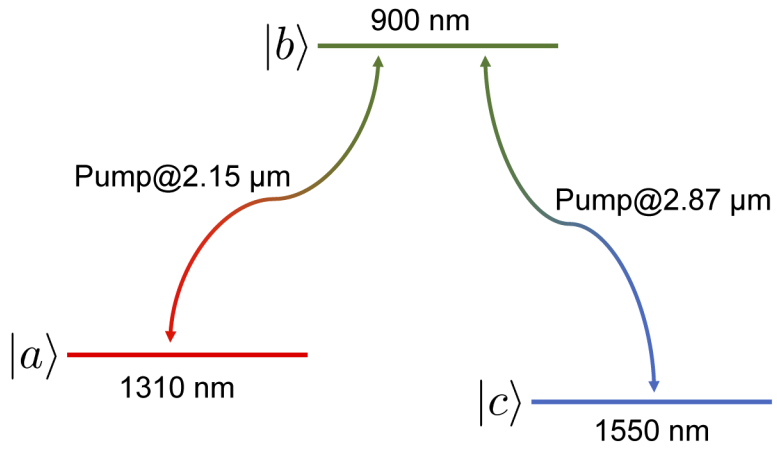

Fig. 4. Effective level configuration for STIRAP-like frequency conversion between telecommunication bands.

full population transfer between the target fields, coupling with pump fields should change during propagation. One can implement such controllable change by sending the pumps through two separate waveguides whose transverse position changes with the propagation coordinate. Target fields propagate in a central waveguide. The conceptual waveguide design is shown in Fig. 5 at the bottom. In this model we used that $\lambda_{a,b,c} \ll \lambda^{\text{pump}}_{a\leftrightarrow b,b\leftrightarrow c}$ so one can neglect coupling of the fields a, b, c to adjacent linear waveguides delivering pump fields to the NLWG. Here for simplicity, we assumed that evanescent coupling between the waveguides are the same for both pump fields ($\lambda^{\text{pump}}_{a\leftrightarrow b} \approx \lambda^{\text{pump}}_{b\leftrightarrow c}$). The numerical simulation results are shown in Fig. 5. Nonlinear coupling strengths are approximately the same as in the EIT model. Alternatively, a propagation-dependent TWM interaction with pump fields can be implemented, for instance, by changing the amplitudes of the Fourier components of the QPM grating along the length of a single waveguide. The desired interaction envelope can be achieved with a Fourier design technique straightforwardly [42].

In addition to enhancing the range of low-noise frequency conversion, the proposed device offers the advantage of unique STIRAP robustness that distinguishes this approach from the "intuitively" ordered sequence of π-pulses [43]. Indeed, the π-pulse sequence is very sensitive to pump parameters and waveguide imperfections.

4.3. Complex quantum systems

By increasing the number of photons n and spectral modes M, one can effectively increase the number of possible states and the effective dimensionality of the waveguide array. Effective number of dimensions can be calculated as the number of possible combinations to distribute n photons over M different modes. Note that this photonic platform is similar to an array of linearly coupled waveguides [21], however we take advantage of an extra degree of freedom, i.e. the spectral domain. The hamiltonian for the array of N coupled nonlinear waveguides, supporting M different quantized spectral modes and up to $M(M-1)$ classical strong pumps (to couple all spectral modes pairwise), can be written as:

$$\hat{H} = \hat{H}_0 + \hat{H}_{\text{int}},$$

where

$$H_0 = \sum_{\substack{j=1,N \\ m=1,M}} k_j^m a_j^{m\dagger} a_j^m$$

Optics EXPRESS

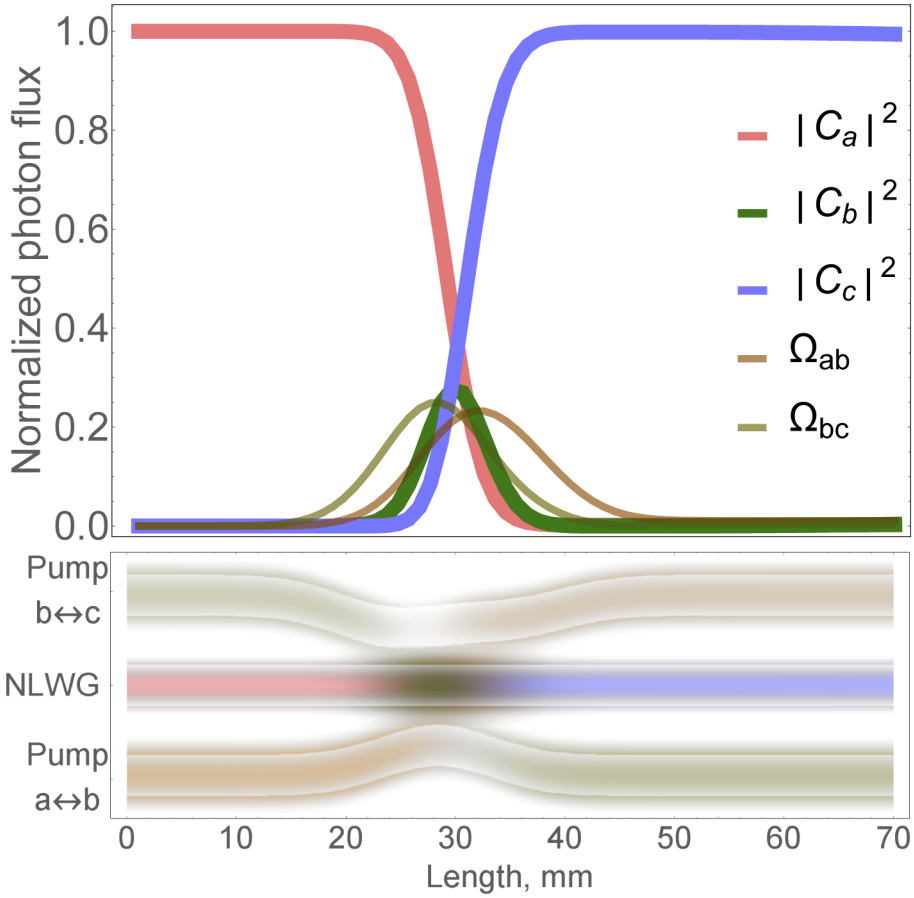

Fig. 5. A numerical simulation of photon flux for all-optical STIRAP frequency conversion implemented with 3 coupled waveguides. The central nonlinear waveguide is the carrier of the target fields. Side waveguides deliver pump fields. The bottom plot shows a conceptual layout of waveguides in the proposed experimental implementation; color gradients are used for the artistic representation of optical fields. Simulation parameters are chosen such that nonlinear couplings are $\Omega_{ab}^{\max} \approx 0.2$ mm^{-1} and $\Omega_{bc}^{\max} \approx 0.25$ mm^{-1} for pump powers of 200 mW.

Optics EXPRESS

is the Hamiltonian of non-interacting modes with propagation constants k_j^m, corresponding to photons in waveguide j and spectral mode m. The interaction Hamiltonian reads:

$$\begin{aligned} H_{\text{int}} &= \sum_{\substack{j=1,N \\ 1\le m<l\le M}} \left(P_j^{lm}(z) e^{-i\Delta k_j^{lm} z} a_j^{m\dagger} a_j^l + h.c. \right) \\ &+ \sum_{\substack{j=1,N \\ m=1,M}} \left(C_{j,j+1}^m a_j^{m\dagger} a_{j+1}^m + C_{j,j-1}^m a_j^{m\dagger} a_{j-1}^m + h.c. \right), \end{aligned} \tag{6}$$

where P_j^{lm} are the coupling coefficients between m^{th} and l^{th} spectral modes due to TWM processes in the j^{th} nonlinear waveguide with the phase mismatch Δk_j^{lm}. $C_{j,j\pm1}^m$ are the coupling constants between m^{th} spectral modes in the neighboring waveguides. Dependence of P_j^{lm} coefficients on propagation coordinate z is due to possible evanescent tunneling of pump fields to the neighbor waveguides. The pump field evolution in the undepleted pump approximation is driven by the coupling between the waveguides only:

$$i\partial_z P_j^{lm} = -C_{j,j+1}^{lm} P_{j+1}^{lm} - C_{j,j-1}^{lm} P_{j-1}^{lm},$$

where $C_{j,j\pm1}^{lm}$ are coupling constants for the pump field to neighbor waveguides.

The Hamiltonian (6) describes a 2D photonic lattice, however, the 2$^{\text{nd}}$ dimension is synthetic, i.e. due to different frequency modes within the 1-dimensional nonlinear waveguide array. In contrast to the passive evanescent field coupling between nearest-neighbor waveguides, TWM-mediated coupling in the synthetic spectral dimension enables a reconfigurable, tunable system. One can engineer a wide variety of Hamiltonians in the frequency domain: from a 1D Ising model with all-to-all coupling to a Honeycomb lattice, from a stub lattice or a dimer lattice to the Floquet system, in which temporal modulations are introduced via the oscillations of the pump field between neighbor waveguides. Therefore, a physical layer of a 1D array of nonlinear waveguides can be extended to a 2D system with the synthetic spectral dimension. In contrast to conventional photonic waveguide arrays, in which the coupling between the waveguides is mostly limited by the nearest neighbors interactions, the quasi-phase-matching in periodically poled waveguides can be engineered to couple all spectral modes. This coupling is controlled by the pump strength. Thus, such a system can be used to simulate complex band structures and topological effects such as “bosonic” superradiance [44].

5. Conclusions

In this work, we have introduced a theoretical formalism in which spatial and spectral modes of classical or quantum single-photon fields are mapped into energy levels of a fictitious atomic system interacting with external optical fields. This formal similarity between all-optical systems and well-studied atomic systems is not only of the fundamental interest of the theoretical quantum optics, but it enables new interesting applications and experimental simulations of atoms on integrated platform and with all-optical control. This approach is characterized by multiple potential advantages. First, it eliminates many decoherence mechanisms typical for an atom, thanks to the very weak interaction of photons with the environment. Second, it allows simulating quantum optical phenomena with classical light paired with a simple classical measurement, while it is also valid if applied to quantum single-photon fields. Third, the all-optical model of an atomic system can be engineered for any available wavelength of the optical sources, within the optical transparency window of the waveguides (from 0.3 μm to 5 μm for PPLN waveguides). Finally, the fabrication of PPLN waveguides is CMOS - compatible, which potentially allows integration of the electronics, detectors and light sources on the same chip in a scalable architecture.

Optics EXPRESS

To illustrate the potential of our theoretical framework, we also presented two practical photonic applications, based on traditional atomic phenomena. First, we demonstrated how the all-optical analogy of the EIT effect can be used to switch coupling between two adjacent waveguides. Second, we used STIRAP as inspiration for robust and noiseless frequency transduction where direct frequency conversion is not possible.

Funding. Interdisciplinary Scientific and Educational School of Moscow University "Photonic and Quantum Technologies. Digital Medicine"; Russian Science Foundation (19-42-04105).

Acknowledgement. We thank Svetlana Malinovskaya, Alan Migdall, Paul Lett and Nikolai Klimov for a critical review of this manuscript and fruitful discussions. O.V. Tikhonova acknowledges partial financial support of the Russian Science Foundation (RSF) project No.19-42-04105 and the Interdisciplinary Scientific and Educational School of Moscow University "Photonic and Quantum Technologies. Digital Medicine."

Disclosures. The authors declare no conflicts of interest.

References

1. H.-S. Zhong, H. Wang, Y.-H. Deng, M.-C. Chen, L.-C. Peng, Y.-H. Luo, J. Qin, D. Wu, X. Ding, Y. Hu, P. Hu, X.-Y. Yang, W.-J. Zhang, H. Li, Y. Li, X. Jiang, L. Gan, G. Yang, L. You, Z. Wang, L. Li, N.-L. Liu, C.-Y. Lu, and J.-W. Pan, "Quantum computational advantage using photons," Science (2020).
2. K. Luke, P. Kharel, C. Reimer, L. He, M. Loncar, and M. Zhang, "Wafer-scale low-loss lithium niobate photonic integrated circuits," Opt. Express **28**(17), 24452–24458 (2020).
3. C. Wang, M. Zhang, X. Chen, M. Bertrand, A. Shams-Ansari, S. Chandrasekhar, P. Winzer, and M. Lončar, "Integrated lithium niobate electro-optic modulators operating at cmos-compatible voltages," Nature **562**(7725), 101–104 (2018).
4. G. I. Stegeman, D. J. Hagan, and L. Torner, "$\chi(2)$ cascading phenomena and their applications to all-optical signal processing, mode-locking, pulse compression and solitons," Opt. Quantum Electron. **28**(12), 1691–1740 (1996).
5. R. Boyd, *Nonlinear Optics* (Elsevier Science, 2003).
6. D. Bouwmeester, J.-W. Pan, K. Mattle, M. Eibl, H. Weinfurter, and A. Zeilinger, "Experimental quantum teleportation," Nature **390**(6660), 575–579 (1997).
7. P. Kumar, "Quantum frequency conversion," Opt. Lett. **15**(24), 1476–1478 (1990).
8. J. A. Giordmaine and R. C. Miller, "Tunable coherent parametric oscillation in $linbo_3$ at optical frequencies," Phys. Rev. Lett. **14**(24), 973–976 (1965).
9. S. A. Akhmanov, A. I. Kovrigin, A. S. Piskarskas, V. V. Fadeev, and R. V. Khokhlov, "Observation of Parametric Amplification in the Optical Range," Soviet Journal of Experimental and Theoretical Physics Letters **2**, 191 (1965).
10. G. Harder, T. J. Bartley, A. E. Lita, S. W. Nam, T. Gerrits, and C. Silberhorn, "Single-mode parametric-down-conversion states with 50 photons as a source for mesoscopic quantum optics," Phys. Rev. Lett. **116**(14), 143601 (2016).
11. J. Zhao, C. Ma, M. Rüsing, and S. Mookherjea, "High quality entangled photon pair generation in periodically poled thin-film lithium niobate waveguides," Phys. Rev. Lett. **124**(16), 163603 (2020).
12. Y.-H. Cheng, T. Thomay, G. S. Solomon, A. L. Migdall, and S. V. Polyakov, "Statistically background-free, phase-preserving parametric up-conversion with faint light," Opt. Express **23**(14), 18671–18678 (2015).
13. I. A. Burenkov, T. Gerrits, A. Lita, S. W. Nam, L. K. Shalm, and S. V. Polyakov, "Quantum frequency bridge: high-accuracy characterization of a nearly-noiseless parametric frequency converter," Opt. Express **25**(2), 907–917 (2017).
14. P. S. Kuo, J. S. Pelc, C. Langrock, and M. M. Fejer, "Using temperature to reduce noise in quantum frequency conversion," Opt. Lett. **43**(9), 2034–2037 (2018).
15. P. C. Strassmann, A. Martin, N. Gisin, and M. Afzelius, "Spectral noise in frequency conversion from the visible to the telecommunication c-band," Opt. Express **27**(10), 14298–14307 (2019).
16. J. Heng, P. Liu, and Z. Zhang, "Enhanced spectral broadening in an optical parametric oscillator based on a ppln crystal," Opt. Express **28**(11), 16740–16748 (2020).
17. M. Zhang, C. Wang, R. Cheng, A. Shams-Ansari, and M. Lončar, "Monolithic ultra-high-q lithium niobate microring resonator," Optica **4**(12), 1536–1537 (2017).
18. C. Wang, C. Langrock, A. Marandi, M. Jankowski, M. Zhang, B. Desiatov, M. M. Fejer, and M. Lončar, "Ultrahigh-efficiency wavelength conversion in nanophotonic periodically poled lithium niobate waveguides," Optica **5**(11), 1438–1441 (2018).
19. D. N. Christodoulides, F. Lederer, and Y. Silberberg, "Discretizing light behaviour in linear and nonlinear waveguide lattices," Nature **424**(6950), 817–823 (2003).
20. H. B. Perets, Y. Lahini, F. Pozzi, M. Sorel, R. Morandotti, and Y. Silberberg, "Realization of quantum walks with negligible decoherence in waveguide lattices," Phys. Rev. Lett. **100**(17), 170506 (2008).
21. A. Rai, G. S. Agarwal, and J. H. H. Perk, "Transport and quantum walk of nonclassical light in coupled waveguides," Phys. Rev. A **78**(4), 042304 (2008).
22. A. L. Jones, "Coupling of optical fibers and scattering in fibers*," J. Opt. Soc. Am. **55**(3), 261–271 (1965).

Optics EXPRESS

23. S. Longhi, "Classical simulation of relativistic quantum mechanics in periodic optical structures," Appl. Phys. B **104**(3), 453–468 (2011).
24. R. Keil, A. Perez-Leija, F. Dreisow, M. Heinrich, H. Moya-Cessa, S. Nolte, D. N. Christodoulides, and A. Szameit, "Classical analogue of displaced fock states and quantum correlations in glauber-fock photonic lattices," Phys. Rev. Lett. **107**(10), 103601 (2011).
25. M. Gräfe, R. Heilmann, A. Perez-Leija, R. Keil, F. Dreisow, M. Heinrich, H. Moya-Cessa, S. Nolte, D. N. Christodoulides, and A. Szameit, "On-chip generation of high-order single-photon w-states," Nat. Photonics **8**(10), 791–795 (2014).
26. A. A. Sukhorukov, A. S. Solntsev, and J. E. Sipe, "Classical simulation of squeezed light in optical waveguide arrays," Phys. Rev. A **87**(5), 053823 (2013).
27. A. S. Solntsev and A. A. Sukhorukov, "Path-entangled photon sources on nonlinear chips," Rev. Phys. **2**, 19–31 (2017).
28. E. Travkin, F. Diebel, and C. Denz, "Compact flat band states in optically induced flatland photonic lattices," Appl. Phys. Lett. **111**(1), 011104 (2017).
29. R. Keil, C. Noh, A. Rai, S. Stützer, S. Nolte, D. G. Angelakis, and A. Szameit, "Optical simulation of charge conservation violation and majorana dynamics," Optica **2**(5), 454–459 (2015).
30. S. Longhi, "Jaynes–cummings photonic superlattices," Opt. Lett. **36**(17), 3407–3409 (2011).
31. M. Scully and M. Zubairy, *Quantum Optics* (Cambridge University Press, 1997).
32. A. P. VanDevender and P. G. Kwiat, "Quantum transduction via frequency upconversion (invited)," J. Opt. Soc. Am. B **24**(2), 295–299 (2007).
33. J. S. Pelc, L. Ma, C. R. Phillips, Q. Zhang, C. Langrock, O. Slattery, X. Tang, and M. M. Fejer, "Long-wavelength-pumped upconversion single-photon detector at 1550 nm: performance and noise analysis," Opt. Express **19**(22), 21445–21456 (2011).
34. P. Fisher, M. Villa, F. Lenzini, and M. Lobino, "Integrated optical device for frequency conversion across the full telecom *c*-band spectrum," Phys. Rev. Appl. **13**(2), 024017 (2020).
35. K. R. Parameswaran, J. R. Kurz, R. V. Roussev, and M. M. Fejer, "Observation of 99% pump depletion in single-pass second-harmonic generation in a periodically poled lithium niobate waveguide," Opt. Lett. **27**(1), 43–45 (2002).
36. D. Marcuse, *Theory of Dielectric Optical Waveguides* (Elsevier Science, 2013).
37. M. H. Chou, K. R. Parameswaran, M. M. Fejer, and I. Brener, "Multiple-channel wavelength conversion by use of engineered quasi-phase-matching structures in linbo3 waveguides," Opt. Lett. **24**(16), 1157–1159 (1999).
38. M. Asobe, O. Tadanaga, H. Miyazawa, Y. Nishida, and H. Suzuki, "Multiple quasi-phase-matched linbo3 wavelength converter with a continuously phase-modulated domain structure," Opt. Lett. **28**(7), 558–560 (2003).
39. M. C. Rechtsman, J. M. Zeuner, Y. Plotnik, Y. Lumer, D. Podolsky, F. Dreisow, S. Nolte, M. Segev, and A. Szameit, "Photonic floquet topological insulators," Nature **496**(7444), 196–200 (2013).
40. M. Jankowski, C. Langrock, B. Desiatov, A. Marandi, C. Wang, M. Zhang, C. R. Phillips, M. Lončar, and M. M. Fejer, "Ultrabroadband nonlinear optics in nanophotonic periodically poled lithium niobate waveguides," Optica **7**(1), 40–46 (2020).
41. T. A. Huffman, G. M. Brodnik, C. Pinho, S. Gundavarapu, D. Baney, and D. J. Blumenthal, "Integrated resonators in an ultralow loss si3n4/sio2 platform for multifunction applications," IEEE J. Sel. Top. Quantum Electron. **24**(4), 1–9 (2018).
42. J. Huang, X. P. Xie, C. Langrock, R. V. Roussev, D. S. Hum, and M. M. Fejer, "Amplitude modulation and apodization of quasi-phase-matched interactions," Opt. Lett. **31**(5), 604–606 (2006).
43. B. W. Shore, "Picturing stimulated raman adiabatic passage: a stirap tutorial," Adv. Opt. Photonics **9**(3), 563–719 (2017).
44. M. Delanty, S. Rebic, and J. Twamley, "Superradiance of harmonic oscillators," (2011).